

INFLUENCE OF THE SWIRLED ELECTROVORTEX FLOW ON THE MELTING OF EUTECTIC ALLOY In-Ga-Sn

Y. Ivochkin, I. Teplyakov, A. Guseva, D. Vinogradov

*Joint Institute for High Temperatures Russian Academy of Sciences,
125412 Moscow, 13-2 Izhorskaya str., Russia e-Mail: vortex@iht.mpei.ac.ru*

It was shown by experimental and computational methods that the process of metal melting essentially depends on the intensity and hydrodynamic structure of electrovortex flows (EVF) developing in a smelting furnace. It was found that by controlling the EVF applying an external longitudinal magnetic field one can reduce the melting time.

List of symbols.

B	magnetic field induction, [T]
F	Amperes force, [N/m ³]
J	electric current density, [A/m ²]
I	electric current, [A]
t	time, [min]
σ	conductivity, [S/m]
Φ	electric potential, [V]

Introduction. The so-called electrovortex flow (EVF) is formed by the interaction of an electric current, spreading into a current-carrying fluid volume, with its self magnetic field [1]. Most of complete experimental and theoretical investigations had been carried out at the Institute of Physics, University of Latvia, under the guidance of E. Shcherbinin. It is assumed that under natural conditions an electrovortex flow as well as free convection [2] may be the cause of hydrodynamic structures similar to a tornado. In technology, intensive EVFs are observed in various high-current technological processes, for example, in electro-arc or electroslag remelting of metal [3]. The hydrodynamic structure of EVF was most fully investigated by numerical methods for working models of melting baths with axisymmetric geometry, in which electrodes of different diameters were located at the butt-ends of the cylindrical shape container [3–5]. In [6], the pioneering measurements of the velocity fields of electrovortex flows had been made in a cylindrical working section, the results of which indicated their complex multi-vortex structure. In subsequent studies [7–9] concerned with the study of electrovortex flows formed at the axisymmetric distribution of the electric current from a point source in a hemispherical volume filled with a liquid metal, it has been experimentally shown that the hydrodynamic structure of EVT is substantially determined by the intensity and orientation of external, even relatively weak magnetic fields acting on the experimental setup. In particular, it has been proven by experimental and computational methods that the paradoxical spontaneous horizontal swirl of the axisymmetric electrovortex flow in a hemispherical bath is caused by the interaction of the electric current, passing in a liquid metal, and the Earth's magnetic field.

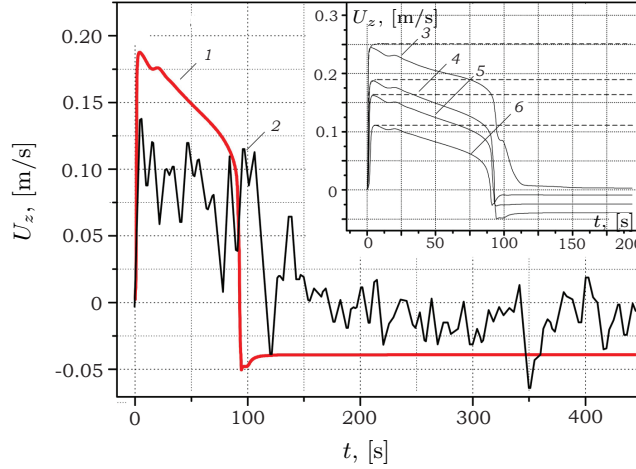


Fig. 1. Oscillograms of the axial velocity on the axis at different depths z . $I = 400$ A; 1 – experiment with FOT, $z = 11.5$ mm; 2 – calculation, $z = 5$ mm; 3 – 11.5 mm; 4 – 15 mm; 5 – 20 mm; 6 – 50 mm.

Furthermore, it has been found experimentally and confirmed numerically that the intensive swirling flow around the horizontal axis of the bath, due to the influence of the external longitudinal magnetic field leads to the formation of secondary vortices in the vertical plane and to suppression of the downward flow in the volume of a current-carrying fluid, except for a small region near the small electrode. The oscillograms of the axial velocity measured by a fiber-optical transducer (FOT) [10] are presented in Fig. 1.

Basing on the results of earlier studies, one can assume that the presence of EVFs and the change of their hydrodynamic pattern under the influence of external magnetic fields affect the metal melting process. However, the analysis of the literature has revealed no studies on the quantitative characteristics of this effect. Therefore, we have carried out additional experimental and computational studies on the influence of EVF on electrosmelting of metals; the methods and the results are discussed below.

1. Experimental setup and measurement procedure. Experiments on the simulation of EVF applied to the electro-arc remelting process were carried out in the setup shown in Fig. 2. A eutectic indium-gallium-tin alloy (weight content: Ga – 67%, In – 20.55, Sn – 12.5%, the melting point $+10.5^\circ\text{C}$) was used as the working liquid in the experiments. The alloy filled a copper hemispherical container with a diameter of 188 mm, which also served as a large electrode. The small electrode – a stainless steel cylinder with the diameter 5 mm with the hemispherical end was immersed into the alloy in the middle of the working bath. Physical properties of the alloy are given in [11]. A power source developed on the base of a three-phase AC rectifier ($I \leq 1500$ A) was used to feed the experimental setup. To create an external longitudinal magnetic field, a coil consisting of 15 turns of hollow copper tube (cooled with pumped water) was used. The coil was supplied from a stabilized power source, providing smooth control of DC in the range from 0 to 100 A. This system allowed to produce a magnetic field with the induction $B = 5 \times 10^{-3}$ T in the middle of the working area at a current of 100 A.

Before the experiments, a special coolant (polymethylsiloxane PMS-5) at a temperature of -25°C was poured into a cylindrical cooling bath located in the gap between the working section and the solenoid. In addition, polymethylsiloxane

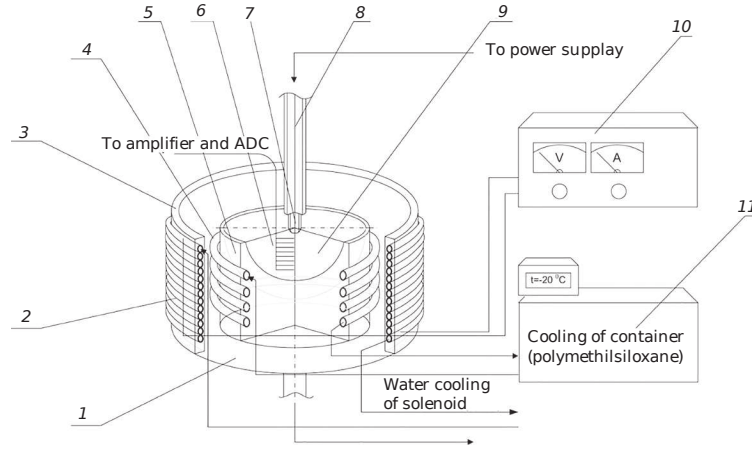


Fig. 2. Experimental setup. 1 – cooling vessel, 2 – water-cooled solenoid, 3 – heat insulation, 4 – heat exchanger, 5 – copper container, 6 – thermocouple probe, 7 – small electrode, 8 – current lead, 9 – In-Ga-Sn, 10 – power supply of solenoid, 11 – refrigerator.

was pumped through the heat exchanger (a tube wrapped around the copper container filled with the alloy). These preliminary procedures allowed to cool In-Ga-Sn to 0°C (at the environment temperature 25°C), i.e. substantially below its freezing temperature of ~10°C. As soon as the liquid solidified in the whole volume of the hemispherical container, polymethylsiloxane was poured away from the cooling bath. Then an electric current was passed through the working area, and heating and melting of liquid metal took place. A probe-comb consisting of 8 chromel-alumel thermocouples with the junction diameter 0.5 mm was used to get thermograms in the volume of the alloy. The width and depth of the molten zone were measured by a special probe.

2. Calculation method. In a numerical study of the influence of EVF on the metal melting process, the so-called enthalpy-porous model built-in software package ANSYS Fluent was used [12]. In this model, a two-phase liquid-solid zone is considered as a porous medium with the porosity equal to the proportion of the liquid phase, and the pressure loss caused by the presence of not molten material was taken into account by introducing an additional dissipative term into the motion equation. The system of conservation equations of momentum, enthalpy and continuity was solved in a non-induction approximation, i.e. the influence of the magnetic field on the velocity field and temperature was taken into account by adding the Ampere force $\mathbf{F} = \mathbf{j} \times \mathbf{B}$ in the motion equation.

To determine the current density \mathbf{j} in all elements of the working area, including both electrodes, the equation for the electric potential Φ ($\text{div}(\sigma \text{grad } \Phi) = 0$) was solved with boundary conditions at the upper and lower end of the current leads $\Phi = \Phi_0$ and $\Phi = 0$, corresponding to a complete electrical current passing through the setup. The current density \mathbf{j} was calculated from the expression $\mathbf{j} = -\sigma \text{grad } \Phi$. A more complete description of the calculation of the magnetic fields and forces acting on the electrically conducting liquid is presented in [13]. Upon solving the motion equation, no-slip conditions were set on all surfaces, including the open surface of the metal because a solid oxide film was formed on it. For the energy equation on the borders with the air, free convection conditions were set, and the temperature of the environment was assumed to be 25°C.

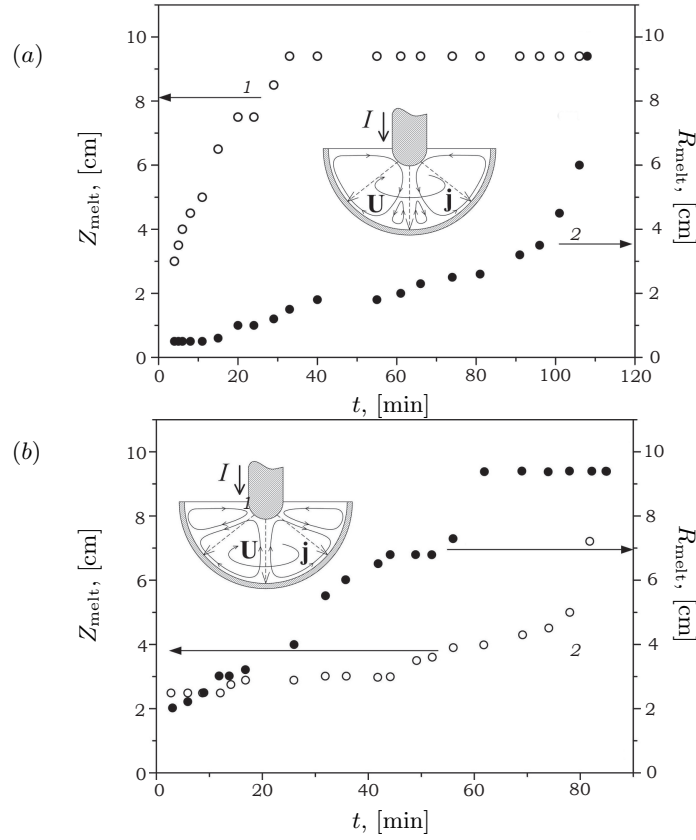


Fig. 3. Moving the melting front in the direction of the axis of the metal bath and radially on its surface. $I = 400$ A. Influence of (a) the (EMF ($B \sim 5 \times 10^{-5}$ T); (b) the EMF and the solenoid $B_{\text{ext}} = 5 \times 10^{-3}$ T. 1 and 2 – coordinates of melting point on the axis and radius of the bath.

3. Results. Typical results of the experimental studies on the distribution of the melting front deep down into the bath and the metal surface are shown in Fig. 3. Shapes of the melting curve boundary at different times in the whole volume of the metal are shown in Fig. 4. Experiments were carried out with the current $I = 400$ A in the presence of the Earth's natural magnetic field (EMF), adding there an artificially created longitudinal (relative to the axis of the setup) magnetic field of the solenoid with the induction $B = 5 \times 10^{-3}$ T. Table 1 lists some data on the rate and time of melting.

As seen from these graphs, there is a significant difference in shape of the melting front under the artificially generated external magnetic fields and in its absence.

In the first case, the shape of this curve follows the shape of the melting pool, and under the influence of the EMF the melting front has a typical shape elongated along the axis of the bath. Also, the time of complete melting of the metal in the bath under the influence of the external magnetic field was by 12% lower than in its absence.

By analyzing the obtained results, one can assume that the process of melting in the processing bath is as follows. At the start of heating of the metal by the electric current, a small portion of the metal near the small electrode melts.

An EVF occurs in the molten liquid volume, and in the ideal case, in the

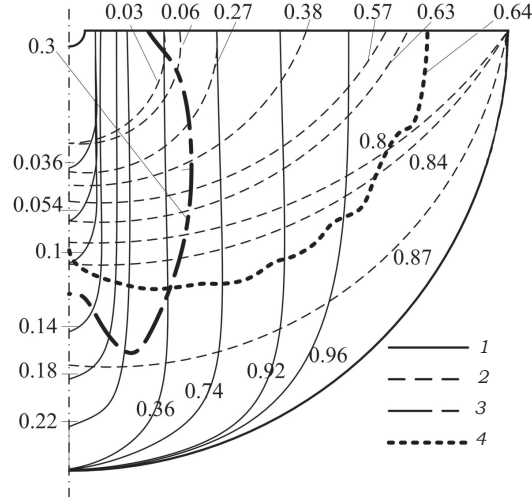


Fig. 4. Melting front distribution with the EMF and without. $I = 400$ A. The numbers on the lines - time from the beginning of the experiment divided by the time of full metal melting. 1 - experiment with $B_{\text{ext}} = 0$; 2 - $B_{\text{ext}} = 5 \times 10^{-3}$ T; 3 - calculation with $B_{\text{ext}} = 0$; 4 - $B_{\text{ext}} = 5 \times 10^{-3}$ T.

Table 1.

	Total melting time	Average melting rate along the Z-axis	Average melting rate along the R-axis
With magnetic field $B = 5 \times 10^{-3}$ T	1 h 38 min	0.10 cm/min	0.14 cm/min
Without magnetic field	1 h 50 min	0.24 cm/min	0.09 cm/min

absence of EMF, the EVF is a single axisymmetric toroidal curl, creating a jet axial flow under the small electrode [1]. The influence of EMF results [8] in an azimuthal rotation which develops in the current-carrying liquid. This movement of the melt in the horizontal plane leads to the generation of a secondary vertical vortex near the bottom area which, although directed opposite to the EVT and due to its relatively low intensity, has no significant effect on the original structure of the EVF (see Fig. 3a). The hot melt flow causes intense melting of the metal in the direction of the Z-axis, and melting in the R-axis direction became noticeable only when the liquid phase of the metal reached the bath bottom. Under the influence of the external longitudinal magnetic field of the solenoid, an azimuthal swirl of the liquid also occurred in the horizontal plane in the working bath, but this swirl was more intense than the one under the influence of EMF. This rotation leads to the generation of a strong secondary vortex in the vertical plane, moving the melt upward along the axis of the working area, and to weakening of the primary EVF (Fig. 3b). Moreover, the intense azimuthal motion of the fluid enhanced the heat and mass transfer processes in the horizontal plane, thereby increasing the metal melting rate in the radial (in the cylindrical coordinates) direction.

The results of numerical calculations (see Fig. 4) are qualitatively consistent with the results of experiments and confirm the melting flow processes described above. The observed quantitative differences can be explained, in particular, by some uncertain parameters (e.g., the value of effective porosity in the mushy zone).

Also, the considerable complexity of the calculations should be noted because the duration of a calculation of one melting mode using the PC with a 4-cores processor was more than one month.

4. Conclusions. As a result of the experimental and numerical studies, it has been found that the impact of the steady axial (longitudinal) magnetic field results in intensification of the melting processes and in reduction of the melting time. The mechanism of this phenomenon is determined by the occurrence of the azimuthal swirl of the melt under these conditions and by the essential transformation of the flow in a hemispherical bath with a central electrode. The hydrodynamic structure of flows formed in the working bath provides a more intensive (due to the formation of additional reverse flows) removal of the heat from the hot region near the small electrode deep into the melt. Furthermore, due to the occurrence and interaction of additional large eddy patterns, the direction of the dominating EVF changes. For this reason, the melting front loses axial direction and gets a radial direction.

Two important practical circumstances must be noted. First, the way to induce external magnetic fields near the melting units with a solenoid is the simplest method. Second, many baths of industrial arc furnaces have horizontal orientation (the ratio of diameter to depth is $\sim 5:1$). Therefore, it can be assumed that the phenomenon described above can be used in these devices to intensify the melting process in the radial direction and enhance its energy efficiency.

Acknowledgements. This work was supported by RSCF, grant No. 14-50-00124. The authors would like to thank Dr. I. Protokovilov and Dr. Yu. Tokarev for useful discussion.

REFERENCES

- [1] V. BOJAREVICH, J. FREJBERGS, E.I. SHILOVA, E.V. SHCHERBININ. *Electrically Induced Vortical flows* (Kluwer Academic Publishers, Dordrecht, Boston, London, 1989).
- [2] A.Y. VARAKSIN, M.E. ROMASH, V.N. KOPEITSEV. Effect of net structures on wall-free non-stationary air heat vortices. *International Journal of Heat and Mass Transfer*, vol. 64 (2013), pp. 817–828.
- [3] YA.YU. KOMPAN, E.V. SHCHERBININ.. *MHD Controlled Electroslag Welding and Smelting* (Mashinostroenie, Moscow, 1989) (in Russ.).
- [4] V.KH. VLASYUK. Turbulent electrovortex flows in a cylindrical space. *Magnetohydrodynamics*, vol. 24 (1988), no. 3, pp. 328–333.
- [5] V.KH. VLASYUK AND E.V. SHCHERBININ. Electrically induced vortical flows in a two-layer fluid. *Magnetohydrodynamics*, vol. 35 (1999), no. 1, pp. 13–20.
- [6] V.G. ZHILIN, YU.P. IVOCHKIN, A.A. OKSMAN, G.R. LURIN'SH, A.I. CHAIKOVSKII, A.YU. CHUDNOVSKII AND E.V. SHCHERBININ. An experimental investigation of the velocity field in an axisymmetric electrovortical flow in a cylindrical container. *Magnetohydrodynamics*, vol. 22 (1986), no. 3, pp. 323–328.
- [7] V. ZHILIN, YU. IVOCHKIN, V. IGUMNOV, A. OKSMAN. Experimental investigation of the electrovortex flows in hemispherical volume. *High Temperature*, vol. 33 (1995), no. 1, pp. 3–6.

- [8] YU. IVOCHKIN, I. TEPLYAKOV, A. GUSEVA, YU. TOKAREV. Numerical and experimental investigation of the swirled electrovortex flow structure. *Thermal Processes in Engineering*, no. 8 (2012), pp. 345–352.
- [9] V.G. ZHILIN, YU.P. IVOCHKIN, I.O. TEPLYAKOV. The problem of swirling of axisymmetric electrovortex flows. *High Temperature*, vol. 49 (2011), no. 6, pp. 927–929.
- [10] V.G. ZHILIN. *Optical-Fiber Velocity and Pressure Transducers* (Hemisphere Publishing Corporation, New York, 1990).
- [11] V.YA. PROKHORENKO, E.A. RATUSHNYAK, B.I. STADNYK, V.I. LAKH, AND A.M. KOVAL. Physical properties of thermometric alloy In-Ga-Sn. *High Temperature*, vol. 8 (1970), no. 2, p. 374.
- [12] V.R. VOLLER AND C. PRAKASH. A fixed-grid numerical modeling methodology for convection-diffusion mushy region phase-change problems. *Int. J. Heat Mass Transfer*, vol. 30 (1987), pp. 1709–1720.
- [13] YU. IVOCHKIN, I. TEPLYAKOV, A. GUSEVA, E. LOZINA, I. KLEMETYEVA, YU. TOKAREV. Investigation of the free surface deformation and its influence to intensity of electrovortex flow of liquid metal. *Thermal Processes in Engineering*, no. 11 (2012), pp. 487–495.

Received 22.12.2014